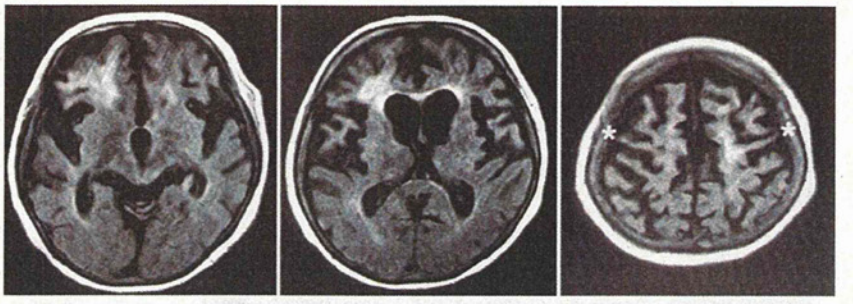

Fig. 1 Fluid-attenuated inversion recovery (FLAIR) images obtained from case 1 about 11 weeks before death. Atrophy of the frontal lobe, particularly the precentral gyrus, is evident, with dilatation of the lateral and third ventricles and enlargement of the sylvian fissure. The basal ganglia also appear atrophic. Asterisks indicate the bilateral precentral gyri.

monoclonal anti-pTDP-43 antibody (pS409/410; 1:2000). Protein concentration was measured by the Bradford method and equal amounts of protein were loaded in each lane.

Sequencing of the *TDP-43* gene

In both cases, high-molecular-weight genomic DNA was extracted after obtaining informed consent from the patients' relatives. We amplified all the exons of *TDP-43* (NM 007353) with use of a series of primers, followed by sequence reaction. This study was approved by the Institutional Review Board of the University of Niigata, Japan.

RERULTS

Case reports

Case 1

A 54-year-old Japanese woman became aware of a decrease in the grasping power of her right hand. Subsequently, she developed difficulty in walking and needed to use a wheelchair. Two months later, she visited a hospital, where examination revealed gait disturbance due to spasticity of the right leg. No muscle atrophy was evident. All the tendon reflexes were hyperactive in the extremities, and Babinski's sign was present on both sides. MRI showed no apparent abnormalities in the brain. Thereafter, the gait disturbance worsened gradually, and at the age of 55 the patient was admitted to Niigata University Hospital for neurological evaluation. On examination, she showed spasticity in the right leg. Lower motor neuron signs were not evident. However, 1 month later, electromyography (EMG) showed a neurogenic pattern in the tongue and limb muscles. Thereafter, dysphagia appeared and progressed gradually, necessitating the introduction of tube feeding.

At the age of 57, the patient was transferred to Nishi-Niigata Chuo National Hospital for medical care and recuperation. She presented with anarthria; an accurate examination of dementia was impossible. Severe muscle weakness, spasticity and markedly increased tendon reflexes were evident in the extremities. Mild muscle atrophy was observed in the tongue. Mild fasciculation was also noted in the right palm and left thigh. MRI showed evident atrophy of the frontal lobe, as well as the anterior part of the temporal lobe, where 123I-IMP single-photon-emission computed tomography (IMP-SPECT) demonstrated hypoperfusion. A further MRI examination revealed progression of the cerebral atrophy (Fig. 1). At the age of 60, the patient developed abdominal distension with high fever for 2 weeks and died.

The final clinical diagnosis was upper-motor-predominant ALS with frontotemporal atrophy.[14] A general autopsy was performed about 3 h after death, at which time the brain weighed 960 g. The cause of death was diffuse peritonitis due to perforation of a stomach ulcer.

Case 2

The clinicopathology of this case has been reported previously.[14] Briefly, a 75-year-old Japanese woman developed slowly progressive upper motor neuron signs, including pseudobulbar palsy manifesting hypophonia (anarthria), increased tendon reflexes and positive Babinski's sign, in the absence of lower motor neuron signs. In the later stage, at the age of 81 years, mutual communication became impossible (she was suspected to have dementia). Frontotemporal cerebral atrophy was evident on MRI. At the age of 82, the patient died of sudden respiratory arrest.

The final clinical diagnosis was atypical MND (including PLS); the cause of frontotemporal atrophy remained uncertain. A general autopsy was performed 3.5 h after death, at which time the brain weighed 883 g. Her death appeared to be attributable to bronchopneumonia of both lungs.

Neuropathological findings

In both cases, atrophy was evident in the frontal lobe, especially in the precentral gyrus (Fig. 2). In addition, the anterior and medial temporal lobes appeared atrophic. In sections, marked atrophy of the precentral gyrus, a decrease in the volume of the centrum semiovale, and dilatation of the lateral ventricle were confirmed (Fig. 3a). There was no evident atrophy of the spinal cord or nerve roots.

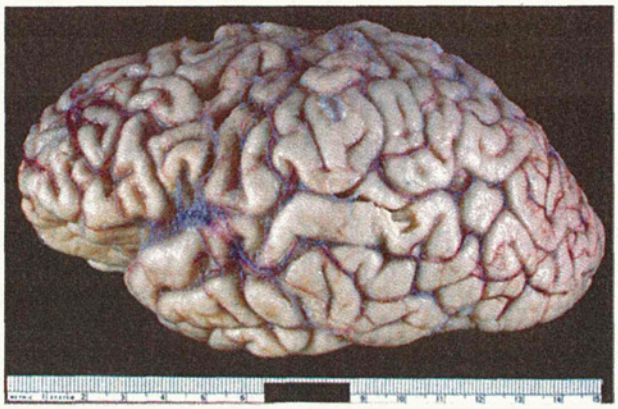

Fig. 2 Case 1. Atrophy is evident in the frontal lobe (the precentral gyrus appears to be most severely affected). In this lateral view, the temporal lobe appears well preserved.

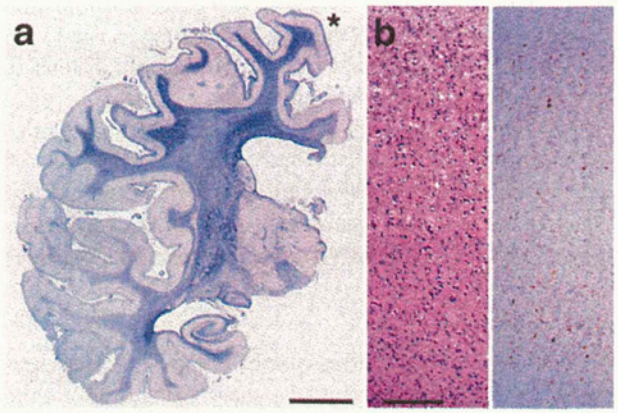

Fig. 3 Case 1. (a) Coronal section through the lateral geniculate body, showing marked atrophy of the precentral gyrus (asterisk). The medial temporal lobe also appears somewhat atrophic. Marked fibrillary gliosis is evident in the frontal and parietal white matter, especially in subcortical white matter. (b) Severe neuronal loss with gliosis was evident in the motor cortex. Note tissue rarefaction with microvacuolar change in layers II–III (left). In a serial section immunostained with the anti-pTDP-43 antibody, many pTDP-43-positive structures, including neuronal cytoplasmic inclusions (NCIs) and dystrophic neurites/neuropil threads (DNs/NTs) can be seen mainly in layers II–III and V–VI (right). (a) Holzer; (b) HE (left), phosphorylated TDP-43 (pTDP-43) immunostaining (right). Bars: 10 mm for (a); 200 μm for (b).

The histological findings obtained were essentially the same in both cases: a combination of FTLD with complete loss of Betz cells in the most severely affected motor cortex (Fig. 3b, left), marked degeneration of the pyramidal (corticospinal) tracts (Fig. 4a), and good preservation of the lower motor neuron nuclei in the brainstem and spinal cord (Fig. 4b). In the affected frontal and temporal cortices, diffuse neuronal loss, with microvacuolar change (Fig. 3b, left) and ubiquitin-positive neuronal cytoplasmic inclusions in layer II, were evident. Neuronal loss was also noted in the amygdala and neostriatum (Fig. 4c,d). The features of other brain regions, including the basal nucleus of Meynert and Ammon's horn, especially the CA1-subiculum border zone, were unremarkable.[23,24] The substantia nigra was intact. Degeneration of the pyramidal (corticospinal) tracts in the medulla oblongata and spinal cord was manifested by advanced, marked atrophy with dense fibrillary gliosis (Fig. 4a). In the lower motor neuron nuclei, in one case (case 2),[14] only a few spinal anterior horn cells were found to contain Bunina bodies, which were immunoreactive for cystatin C. In both of the present cases, only a few lower motor neurons were found to contain ubiquitin-positive inclusions. Mild, focal denervating neurogenic changes were observed in the scalenus muscle in one case (case 1; for which the tongue, diaphragm, and scalenus and iliopsoas muscles were examined).

In both cases, no pathological features suggestive of complications arising from tauopathies, including Alzheimer's disease (AD) and argyrophilic grain disease,[25] or α–synucleinopathies, including Parkinson's disease, were evident.

Distribution and severity of pTDP-43 deposits

pTDP-43-positive lesions were found not only in the upper and lower motor neuron systems but also in the non-motor neuron systems of the CNS. In both cases, only a few lower motor neurons were found to contain pTDP-43-positive inclusions in the cytoplasm (neuronal cytoplamic inclusions: NCIs) (Fig. 4e,f). On the other hand, in the affected cerebral cortices, particularly in the premotor/motor area, many NCIs and dystrophic neurites/neuropil threads (DNs/NTs) were found mainly in neurons in layers II–III and V–VI (Fig. 3b, right; Fig. 5a,b). Although no loss of granule cells was noted in the hippocampal dentate gyrus, pTDP-positive NCIs, and DNs/NTs were also found there (Fig. 5c). Here NTs were defined as fine, short filamentous structures similar to those visualized with AT8 in the affected cerebral cortex in patients with AD.

In both cases, occurrence of NCIs and DNs/NTs was also a feature in the amygdala and neostriatum (Fig. 5d). On the other hand, in the globus pallidus, no neuronal loss or pTDP-43-positive NCIs were evident, although pTDP-43-positive coarse granular structures were present in the neuropil (Fig. 5e). Glial cytoplasmic inclusions (GCIs) were occasionally encountered in the above-mentioned affected regions. No pTDP-43-positive lesions were found in the dorsal root or sympathetic ganglia, and no pTDP-43-positive neuronal intranuclear inclusions (NIIs) could be detected in any of the regions examined. In this connection, no FUS pathology was observed (data not shown).[26]

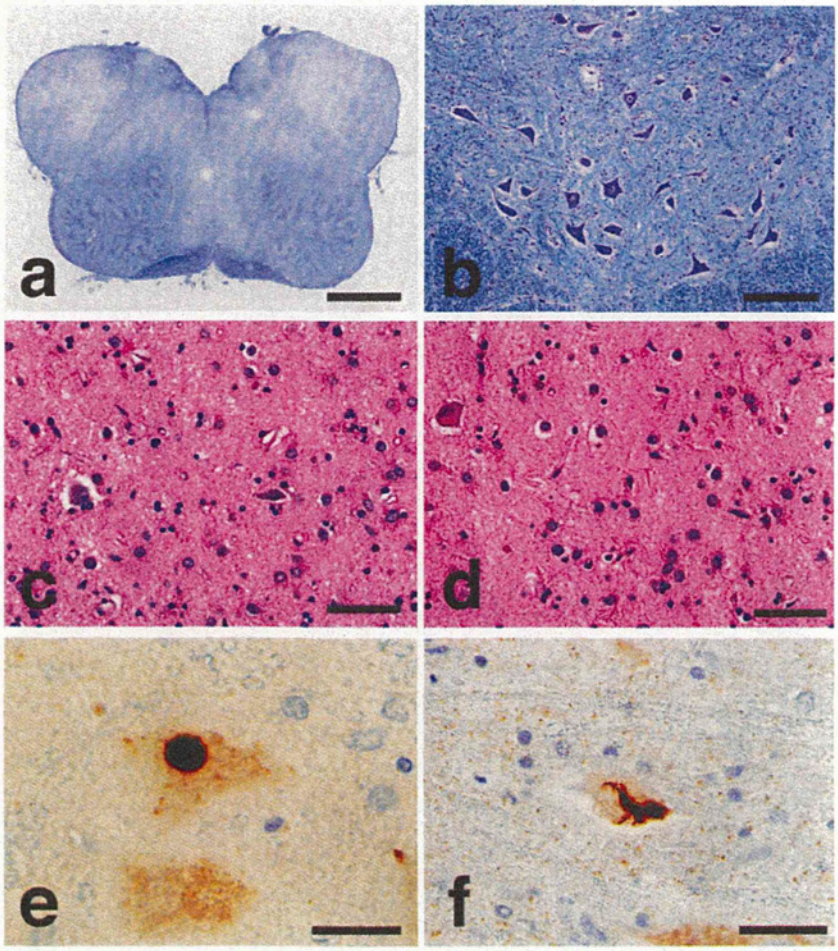

Fig. 4 (a) Marked atrophy with fibrillary gliosis is evident in the bilateral pyramids. (b) No loss of motor neurons is evident in the left lumbar anterior horn. (c, d) Neuronal loss and gliosis are evident in the putamen. (e, f) p-TDP-43-positive round and skein-like neuronal cytoplasmic inclusions (NCIs) in a neuron in the motor nucleus of the trigeminal nerve (e) and a neuron in the cervical anterior horn (f), respectively. (a–c, e) case 1; (d, f) case 2. (a) Holzer; (b) KB; (c, d) HE; (e, f) pTDP-43 immunostaining. Bars: 3 mm for (a); 200 μm for (b); 50 μm for (c, d); 20 μm for (e, f).

The presence of such NCIs, DNs/NTs and GCIs was also detected with the polyclonal antibody against TDP-43, and endogenous nuclear TDP-43 was never recognized by the monoclonal antibody against pTDP-43. The distribution and severity of neuronal loss and pTDP-43 lesions in the CNS are shown in Table 1 (the data sheet introduced by Dickson *et al.*[27] was used with a few modifications). The neuropathological findings obtained in the two patients are summarized in Table 2.

TDP-43 expression analysis

Immunoblotting with the phosphorylation-independent anti-TDP-43 antibody (10782-1-AP) showed bands of ~43 kDa and 45 kDa in both cases (Fig. 6a, upper panel). On the other hand, immunoblotting with the phosphorylation-dependent anti-TDP-43 antibody (pS409/410) revealed that fragments of ~25-kDa were present in the cortices, but not in the spinal cord in both cases (Fig. 6a, lower panel). In addition, the ~25-kDa band patterns differed slightly between the present two cases and the ALS case. Detailed analysis of the pTDP-43 fragments revealed that the band patterns of the 23- and 24-kDa fragments differed between the ALS case and cases 1 and 2: the 24-kDa band was more intense than the 23-kDa band in the ALS case, being consistent with the findings detailed in the previous report,[22] whereas the 23-kDa band was most intense in cases 1 and 2 (Fig. 6b).

TDP-43 gene

Neither of the present cases showed any mutation in the *TDP-43* gene.

DISCUSSION

The two patients examined in the present study had exhibited progressive UMN signs (muscle weakness, hyperreflexia, spasticity and positive Babinski's sign), in the absence of lower motor neuron signs (case 2) or in the presence of only mild lower motor neuron signs appearing later (case 1), followed by progressive frontotemporal atrophy. One patient (case 2) was strongly suspected to have dementia.[14] In both patients, the disease duration was

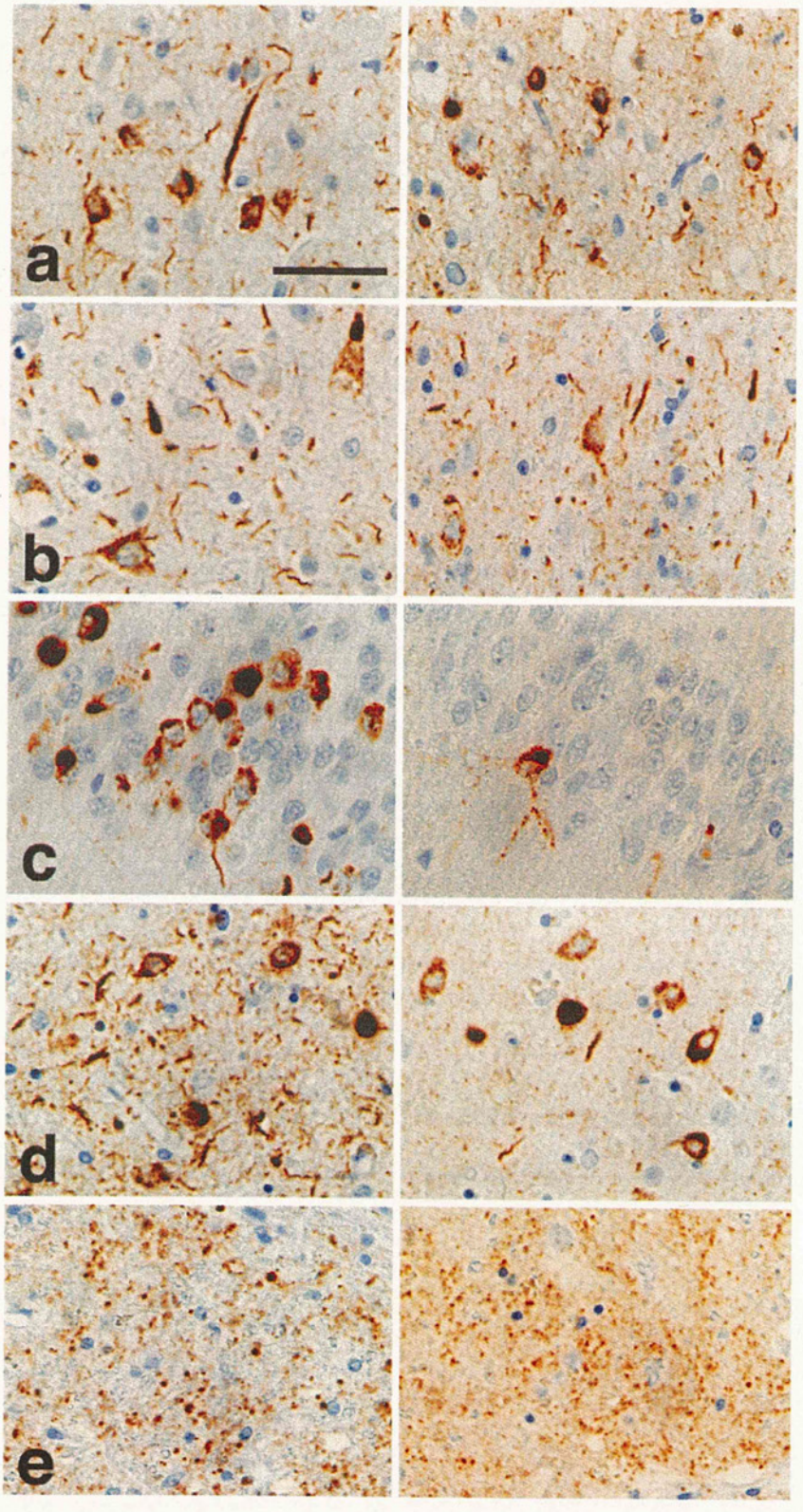

Fig. 5 (a–e) The distribution and severity of pTDP-43 lesions. Here the lesions include neuronal cytoplasmic inclusions (NCIs), dystrophic neurites/neuropil threads (DNs/NTs)and neuropil coarse granules. (a) Precentral cortex layer II; (b) precentral cortex layer V; (c) hippocampal dentate gyrus (granule cells); (d) putamen; (e) globus pallidus (lateral segment). Case 1 (left); case 2 (right). (a–e) pTDP-43 immunostaining. Bar: 40 μm for (a–e).

Table 1 Distribution and severity of neuronal loss and pTDP-43 lesions in the two studied patients

Cases	Neuronal loss		pTDP-43 NCIs		pTDP-43 DNs/NTs		pTDP-43 glia	
	1	2	1	2	1	2	1	2
Anterior olfactory nucleus	0	0	1	0	1	0	1	0
Cerebral cortex								
Frontal	2	1	2	2	2	2	1	1
Premotor/motor	2/2	2/2	2/2	2/2	2/2	2/2	1/1	1/1
Parietal	1	1	2	1	2	1	1	1
Temporal/temporal tip	1/2	1/1	2/2	2/2	2/2	2/2	1/1	1/1
Entorhinal	1	1	1	1	2	1	1	0
Occipital	0	0	1	0	1	1	1	1
Subcortical white matter							0	1
Subcortical areas								
Hippocampus/subiculum	0/0	0/0	1/2	1/2	1/2	1/2	0/1	0/0
Dentate gyrus	0	0	2	1	1	1	0	0
Amygdala	1	0	2	2	1	1	0	0
Basal nucleus of Meynert	0	0	0	0	0	0	0	0
Caudate/putamen	2/2†	1/1†	2/2	2/2	2/2	2/2	1/1	1/1
Globus pallidus	0	0	0	0	2‡	2‡	0	0
Internal capsule							0	0
Thalamus	1	1	1	0	1	0	0	0
Subthalamic nucleus	ne	0	ne	1	ne	1	ne	0
Brainstem								
Superior colliculus	ne	ne	ne	ne	ne	ne	ne	ne
Periaqueductal gray	0	0	0	0	1	0	0	0
Red nucleus	0	ne	1	ne	2	ne	1	ne
Substantia nigra	0	0	0	0	1	1	0	0
Cerebral peduncle							0	0
Pontine tegmentum	0	0	0	0	1	1	0	0
Pontine nuclei	0	0	1	1	1	1	0	0
V/VII/XII	0/0/0	ne/0/0	1/1/0	ne/0/0	1/1/1	ne/1/1	1/0/0	ne/0/0
Inferior olivary nuclei	0	0	0	0	1	2	0	0
Pyramid							0	0
Cerebellum								
Cerebellar cortex	0	0	0	0	0	0	0	0
Dentate nucleus	0	0	0	0	1	0	0	0
Cerebellar white matter							0	0
Spinal cord								
Anterior horns: C/T/L	0/0/0	0/0/0	1/1/0	1/1/1	1/1/1	1/1/1	0/0/0	0/0/0
Intermediate area	0	0	0	0	0	0	0	0
Clarke's column	0	0	0	0	0	0	0	0
Posterior horn	0	0	0	0	0	0	0	0
Spinal white matter							0	0

The presence and severity of neuronal loss, as well as phosphorylated TDP-43 (pTDP-43)-positive neuronal cytoplasmic inclusions (NCIs), dystrophic neurites/neuropil threads (DNs/NTs) and glial cytoplasmic inclusions (GCIs) are represented as: 0 = none; 1 = minimal/mild; 2 = moderate/severe. V/VII/XII, motor nucleus of trigeminal nerve/motor nucleus of facial nerve/hypoglossal nucleus. C/T/L, cervical/thoracic/lumbar. ne, not examined. † Neuronal loss: more marked in the dorsolateral part. ‡ Many pTDP-43-positive coarse granular structures were observed in the neuropil.

[Correction added on 16 April 2012, after first online publication: Midbrain tectum was replaced with Superior colliculus under Brainstem]

more than 5 years;[9,12] in case 1, death was unequivocally attributable to diffuse peritonitis.

Neuropathologically, in both cases, neuronal loss was severe in the motor cortex and degeneration was evident in the descending pyramidal (corticospinal) tracts. On the other hand, neuronal loss was not evident or if present, only mild in the lower motor neuron nuclei, including the spinal anterior horns. However, with regard to the cellular pathology, the occurrence of Bunina bodies and/or ubiquitin inclusions was a feature of the lower motor neurons in both cases. It was also noteworthy that degeneration with ubiquitin inclusions seen in the motor cortex was found to extend to the other frontal cortices anteriorly, as well as to the temporal cortices ventrally. In both cases, the final neuropathogical diagnosis was "upper-motor predominant ALS with FTLD-U".[14] The entire clinicopathological picture was different from that seen in known variants of ALS, including typical ALS,[30] ALS of long duration,[31] or ALS with dementia (ALS-D) or FTLD with MND (FTLD-MND).[23,32,33] Patients with ALS of long duration[31] or FTLD-MND[32,33] usually show the neuropathology of lower-motor-predominant ALS.

In the present study, we also carried out a systematic examination of the distribution and severity of pathologi-

Table 2 Summary of pathological findings in the two studied patients

	Case 1	Case 2
Brain weight (g)	960	883
Upper-motor neuron system		
Loss of Betz cells	+ (complete)	+ (complete)
Degeneration of pyramidal tract	+ (advanced, severe)	+ (advanced, severe)
pTDP-43 inclusions (NCIs and DNs/NTs)	+	+
Lower-motor neuron system		
Neuronal loss (V/VII/XII/SAH)	–/–/–/–	ne/–/–/–
Bunina bodies (V/VII/XII/SAH)	–/–/–/–	ne/–/–/+
Ubiquitin NCIs (SAH)	+	+
pTDP-43 NCIs (V/VII/XII/SAH)	+/+/–/–	ne/–/–/+
Frontal and temporal lobes		
Atrophy and degeneration	+ (frontal > temporal)	+ (frontal > temporal)
Ubiquitin NCIs	+	+
pTDP-43 inclusions (NCIs and DNs/NTs)	+	+
FTLD-TDP (pathological/biochemical)	*Type A*†/Type 1‡	*Type A*†/Type 1‡
Subcortical gray (amygdala/neostriatum)		
Neuronal loss	+/+	+/+
pTDP-43 inclusions (NCIs and DNs/NTs)	+/+	+/+
Neurogenic muscular atrophy	+ (mild, scalenus muscle)	–

pTDP-43, phosphorylated TDP-43; NCIs, neuronal cytoplasmic inclusions; DNs/NTs, dystrophic neurites/neuropil threads; V/VII/XII/SAH, motor nucleus of trigeminal nerve/motor nucleus of facial nerve/hypoglossal nucleus/spinal anterior horns; FTLD, frontotemopral lobar degeneration. +, present; –, absent; ne, not examined. † The nomenclature recommended by Mackenzie *et al.* was used.[28] ‡ The pTDP-43 band pattern was similar to that of "Type 1" shown by Arai *et al.*[29]

cal pTDP-43 lesions. Both of our patients had many pTDP-43-positive NCIs in the frontal and temporal cortex, amygdala, and neostriatum, where occurrence of many associated DNs/NTs was also evident. Occurrence of many pTDP-43-positive NCIs in the dentate granule cells was also observed in one case (case 1). In contrast to the frontotemporal cortex, occurrence of pTDP-43-positive NCIs and DNs/NTs was not conspicuous in the brainstem and spinal cord; in both cases, only a few lower motor neurons were found to contain NCIs.

In the context of FTLD, the present cases were readily classifiable as FTLD-TDP. However, it was somewhat difficult to subclassify them further: the present cortical TDP-43 pathology manifested by many NCIs and many DNs/NTs, but no NIIs was finally considered "*Type A*[28] (Type 1,[34] Type 3[35])". In this subtype *Type A*,[28] the occurrence of NIIs is regarded as an inconsistent feature. In this connection, in the two cases, although the occurrence of pTDP-43 NCIs was minimal in the brainstem and spinal cord, the distribution pattern might be fundamentally similar to that of type 2 (Nishihira *et al.*, 2008)[36] seen in sporadic ALS.[37] The *Type A* is reported to be a common phenotype in behavioural variants of frontotemporal dementia and progressive non-fluent aphasia, and in association with the presence of *GRN* (progranulin gene) mutations.[28] It is noteworthy that FTLD-MND (including ALS-D)[38] is usually subclassified as *Type B*[28] (Type 3,[34] Type 2[35]),[39–43] in which the cortical TDP-43 pathology is characterized by moderate NCIs and few DNs (/NTs).[28] We also confirmed a classification of *Type B* in clinicopathologically proven cases of FTLD-MND.[44] Thus, the overall pTDP-43 pathology was also distinguishable from that seen in typical ALS,[36,45] ALS of long duration,[46] ALS-D or FTLD-MND,[39–44] or MND clinically limited to the lower motor neuron system;[47] the clinicopathology of the present cases appears to add a new variant, "PLS: upper-motor-predominant ALS with FTLD-TDP (*Type A*)[28]", to the single major TDP-43 proteinopathy spectrum involving ALS and FTLD.[48–50]

The results obtained by immunoblot analysis of pTDP-43 also appeared to support this idea. The band pattern of the fragmented ~25-kDa pTDP-43 differed between the present cases and a case of ALS. It has been shown that there is a correlation between the pathological subtypes of TDP-43 proteinopathy and the band pattern of the C-terminal fragments of pTDP-43: a 23-kDa band is most intense in FTLD-TDP, while a 24-kDa band is most intense in FTLD-MND or ALS.[22,29] The band pattern of the C-terminal fragments of pTDP-43 shown in the present study resembled that described for FTLD-U (pathologically Type 1[35]/*Type C*[28]):[22] this band pattern was designated later as "Type 1" by Arai *et al.* (see Fig. 2 in their article).[29] The absence of ~25-kDa fragments of pTDP-43 in the spinal cord in the present cases clearly reflected the neuropathological finding of well-preserved anterior horn neurons, only a few of which contained pTDP-43-positive NCIs.

Dickson *et al.* studied the occurrence of TDP-43 lesions in four patients with corticospinal tract degeneration without lower motor neuron pathology (PLS with or

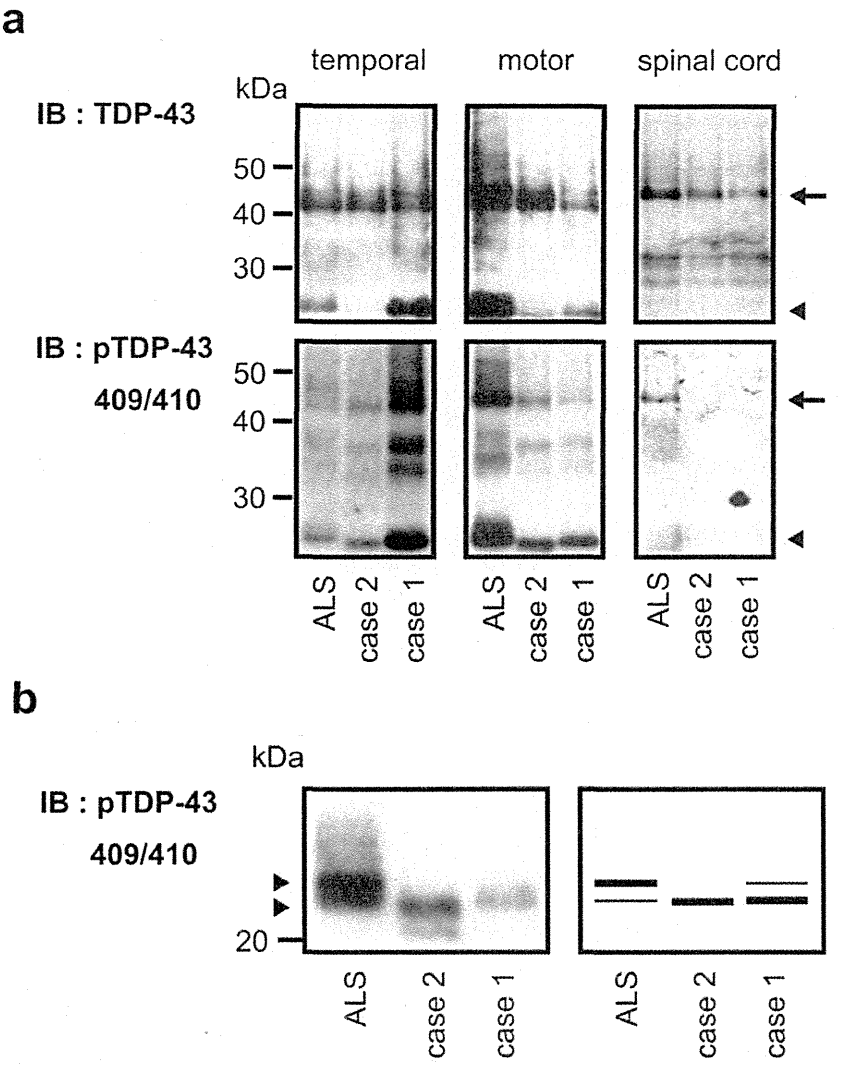

Fig. 6 (a) Immunoblot analysis of the sarkosyl-insoluble, urea-soluble fractions from one amyotrophic lateral sclerosis (ALS) and two primary lateral sclerosis (PLS) (cases 1 and 2) brains (temporal and motor cortices) and spinal cords with anti-TDP-43 (upper panels) and anti-pTDP-43 antibodies (lower panels). Arrows indicate full-length TDP-43 and arrowheads indicate fragmented TDP-43. Note that ~25-kDa bands of pTDP-43 are evident in the brain samples in all cases, but not in the spinal cord samples in the two PLS cases (cases 1 and 2). (b) Detailed immunoblot analysis of the sarkosyl-insoluble, urea-soluble fractions from the ALS and PLS motor cortices with the anti-pTDP-43 antibody (left panel). A 24-kDa band is more intense than a 23-kDa band in the ALS case (Type 2).[29] On the other hand, a 23-kDa band is most intense in the two PLS cases (cases 1 and 2) (Type 1).[29] Diagram of the band pattern of the pTDP-43 fragments is also shown (right panel).

without FTLD).[20] In this study, 5-μm-thick, paraffin-embedded sections of the medulla oblongata were subjected to TDP-43 immunohistochemical investigation using the rabbit polyclonal antibody (10782-1-AP; Protein Tech Group Inc., Chicago, IL, USA; 1:3000). Interestingly, one of two patients with PLS without FTLD had TDP-43-positive inclusions in motor neurons and glia in the hypoglossal nucleus, where no neuronal loss, reactive gliosis or Bunina bodies were evident; unfortunately, no further information was available.[20] Two cases with PLS with FTLD (FTLD-PLS) had no TDP-43 immunoreactivity in either motor or extra-motor neurons, or glia.[20] Subsequently, the authors further studied the ubiquitin and TDP-43 pathology in these two cases that were designated as FTLD-PLS, showing ubiquitin- and TDP-43-positive cytoplasmic inclusions and neurites in the frontal and temporal lobe and in the dentate granule cells of the hippocampus (no comments were made on the classification of the cortical TDP-43 pathology),[21] and in their report they mentioned our previous case[14] as an example of FTLD-PLS.[21] However, it is apparent that in their two cases, cognitive impairment was an initial and cardinal clinical feature; taking this clinical aspect into account, we consider that our case in question is not an example of FTLD-PLS, but rather one of PLS-FTLD. In a recent article dealing with FTLD-TDP, in most cases designated FTLD-PLS, the clinical diagnosis was a tauopathy, Pick's disease.[42]

In conclusion, we have described the neuropathological findings with analysis of pathological pTDP-43 lesions in two cases of PLS[12,14,15] as "a TDP-43 proteinopathy of upper-motor-predominant ALS with FTLD". In both cases, occurrence of many pTDP-43-positive NCIs and DNs/NTs in the frontotemporal cortices, especially the

motor cortex (FTLD-TDP, *Type A*), and selected subcortical grays (amygdala and neostriatum) was a feature. By contrast, in most of the lower motor neuron nuclei, neuronal loss was not evident, although Bunina bodies and/or pTDP-43-positive NCIs were detectable only in a few lower motor neurons. Biochemically, in both cases, the ~25-kDa bands of pTDP-43 were detected in the cortex but not in the spinal cord, and the patterns of the pTDP-43 bands were similar to those described in FTLD-U (TDP) (Type 1),[29] and not ALS or FTLD-MND (Type 2).[29]

ACKNOWLEDGEMENTS

We thank C. Tanda, J. Takasaki, H. Saito, T. Fujita, S. Egawa and S. Nigorikawa for their technical assistance. This work was supported by a grant from the Research Committee for CNS Degenerative Diseases, the Ministry of Health, Labour and Welfare, Japan, Grants-in-Aid, 20240037 and 23240049, for Scientific Research from the Ministry of Education, Culture, Sports, Science, and Technology, Japan, and a Project Research Promotion Grant from the University of Niigata.

REFERENCES

1. Pringel CE, Hudson AJ, Munoz DG, Kiernan JA, Brown WF, Ebbers GC. Primary lateral sclerosis. Clinical features, neuropathology and diagnostic criteria. *Brain* 1992; **115**: 495–520.
2. Fisher CM. Pure spastic paralysis of corticospinal origin. *Can J Neurol Sci* 1997; **4**: 251–280.
3. Younger DS, Chou S, Hays AP *et al.* Primary lateral sclerosis. A clinical diagnosis reemerges. *Arch Neurol* 1988; **45**: 1304–1307.
4. Rowland LP. Primary lateral sclerosis: disease, syndrome, both or neither? *J Neurol Sci* 1999; **170**: 1–4.
5. Swash M, Desai J, Misra VP. What is primary lateral sclerosis? *J Neurol Sci* 1999; **170**: 5–10.
6. Le Forestier N, Maisonobe T, Piquard A *et al.* Does primary lateral sclerosis exist? A study of 20 patients and a review of the literature. *Brain* 2001; **124**: 1989–1999.
7. Gordon PH, Cheng B, Katz IB *et al.* The natural history of primary lateral sclerosis. *Neurology* 2006; **66**: 647–653.
8. Singer MA, Statland JM, Wolfe GI, Barohn RJ. Primary lateral sclerosis. *Muscle Nerve* 2007; **35**: 291–302.
9. Singer MA, Kojan S, Barohn RJ *et al.* Primary lateral sclerosis. Clinical and laboratory features in 25 patients. *J Clin Neuromuscul Dis* 2005; **7**: 1–9.
10. Tartaglia MC, Rowe A, Findlater K, Orange JB, Grace G, Strong MJ. Differentiation between primary lateral sclerosis and amyotrophic lateral sclerosis. *Arch Neurol* 2007; **64**: 232–236.
11. Gordon PH, Cheng B, Katz IB, Mitsumoto H, Lowland LP. Clinical features that distinguish PLS, upper motor neuron-dominant ALS, and typical ALS. *Neurology* 2009; **72**: 1948–1952.
12. Eisen AA. Chapter 16 Primary lateral sclerosis. *Handb Clin Neurol* 2007; **82**: 315–325.
13. Rowland LP. Primary lateral sclerosis, hereditary spastic paraplegia, and mutations in the *alsin* gene: historical background for the first international conference conference. *Amyotroph Lateral Scler* 2005; **6**: 67–76.
14. Tan C-F, Kakita A, Piao Y-S *et al.* Primary lateral sclerosis: a rare upper-motor-predominant form of amyotrophic lateral sclerosis often accompanied by frontotemopral lobar degeneration with ubiquitinated neuronal inclusions. *Acta Neuropathol (Berl)* 2003; **105**: 615–620.
15. Yoshida M. Amyotrophic lateral sclerosis with dementia: the clinicopathological spectrum. *Neuropathology* 2004; **24**: 87–102.
16. Mabuchi N, Watanabe H, Atsuta N *et al.* Primary lateral sclerosis presenting parkinsonian symptoms without nigrostriatal involvement. *J Neurol Neurosurg Psychiatry* 2004; **75**: 1768–1771.
17. Norlinah IM, Bhatia KP, Ostergaard K, Howard R, Arabia G, Quinn NP. Primary lateral sclerosis mimicking atypical parkinsonism. *Mov Disord* 2007; **22**: 2057–2062.
18. Neumann M, Sampathu DM, Kwong LK *et al.* Ubiquitinated TDP-43 in frontotemporal lobar degeneration and amyotrophic lateral sclerosis. *Science* 2006; **314**: 130–133.
19. Arai T, Hasegawa M, Akiyama H *et al.* TDP-43 is a component of ubiquitin-positive tau-negative inclusions in frontotemporal lobar degeneration and amyotrophic lateral sclerosis. *Biochem Biophys Res Commun* 2006; **351**: 602–611.
20. Dickson DW, Josephs KA, Amador-Ortiz C. TDP-43 in differential diagnosis of motor neuron disorders. *Acta Neuropathol (Berl)* 2007; **114**: 71–79.
21. Josephs KA, Dickson DW. Frontotemporal lobar degeneration with upper motor neuron disease/primary lateral sclerosis. *Neurology* 2007; **69**: 1800–1801.
22. Hasegawa M, Arai T, Nonaka T *et al.* Phosphorylated TDP-43 in frontotemporal lobar degeneration and amyotrophic lateral sclersosis. *Ann Neurol* 2008; **64**: 60–70.
23. Nakano I. Frontotemporal dementia with motor neuron disease (amyotrophic lateral sclerosis). *Neuropathology* 2000; **20**: 68–75.

24. Toyoshima Y, Piao Y-S, Tan C-F *et al.* Pathological involvement of the motor neuron system and hippocampal formation in motor neuron disease-inclusion dementia. *Acta Neuropathol (Berl)* 2003; **106**: 50–56.
25. Soma K, Fu Y-J, Wakabayashi K, Onodera O, Kakita A, Takahashi H. Co-occurrence of argyrophilic grain disease in sporadic amyotrophic lateral sclerosis. *Neuropathol Appl Neurobiol* 2011; doi:10.1111/j.1365-2990.2011.01175.x.[Epub ahead of print].
26. Mackenzie IRA, Ansorge O, Strong M *et al.* Pathological heterogeneity in amyotrophic lateral sclerosis with *FUS* mutations: two distinct patterns correlating with disease severity and mutation. *Acta Neuropathol (Berl)* 2011; **122**: 87–98.
27. Dickson DW, Bergeron C, Chin SS *et al.* Office of Rare Diseases neuropathologic criteria for corticobasal degeneration. *J Neuropathol Exp Neurol* 2002; **61**: 935–946.
28. Mackenzie IRA, Neumann M, Baborie A *et al.* A harmonized classification system for FTLD-TDP pathology. *Acta Neuropathol (Berl)* 2011; **122**: 111–113.
29. Arai T, Hasegawa M, Nonoka T *et al.* Phosphorylated and cleaved TDP-43 in ALS, FTLD and other neurodegenerative disorders and in cellular model of TDP-43 proteinopathy. *Neuropathology* 2010; **30**: 170–181.
30. Piao Y-S, Wakabayashi K, Kakita A *et al.* Neuropathology with clinical correlations of amyotrophic lateral sclerosis: 102 autopsy cases examined between 1962 and 2000. *Brain Pathol* 2003; **12**: 10–22.
31. Iwanaga K, Hayashi S, Oyake M *et al.* Neuropathology of sporadic amyotrophic lateral sclerosis of long duration. *J Neurol Sci* 1997; **146**: 139–143.
32. Mitsuyama Y. Presenile dementia with motor neuron disease in Japan: clinico-pathological review of 26 cases. *J Neurol Neurosurg Psychiatry* 1984; **47**: 983–959.
33. Mitsuyama Y, Inoue T. Clinical entity of frontotemporal dementia with motor neuron disease. *Neuropathology* 2009; **29**: 649–654.
34. Mackenzie IR, Baborie A, Pickering-Brown S *et al.* Heterogeneity of ubiquitin pathology in frontotemporal lobar degeneration: classification and relation to clinical phenotype. *Acta Neuropathol (Berl)* 2006; **112**: 539–549.
35. Sampathu DM, Neumann M, Kwong LK *et al.* Pathological heterogeneity of frontotemporal lobar degeneration with ubiquitin-positive inclusions delineated by ubiquitin immunohistochemistry and novel monoclonal antibodies. *Am J Pathol* 2006; **169**: 1343–1352.
36. Nishihira Y, Tang C-F, Onodera O *et al.* Sporadic amyotrophic lateral sclerosis: two pathological patterns shown by analysis of distribution of TDP-43-immunoreactive neuronal and glial cytoplasmic inclusions. *Acta Neuropathol (Berl)* 2008; **116**: 169–182.
37. Fu Y-J, Tan C-F, Nishihira Y, Takahashi H. Pathological TDP-43 in a case of primary lateral sclerosis. *Dement Geriatr Cogn Disord* 2010; **30** (Suppl 1): 37 (abstract).
38. McKhann GM, Albert MS, Grossman M, Miller B, Dickson D, Trojanowski JQ, Work Group on Frontotemporal Dementia and Pick's disease. Clinical and pathological diagnosis of frontotemporal dementia: report of the Work Group on Frontotemporal Dementia and Pick's disease. *Arch Neurol* 2001; **58**: 1803–1809.
39. Brandmeir NJ, Geser F, Kwong LK *et al.* Severe subcortical TDP-43 pathology in sporadic frontotemopral degeneration with motor neuron disease. *Acta Neuropathol (Berl)* 2008; **115**: 123–131.
40. Yokota O, Tsuchiya K, Arai T *et al.* Clinicopathological characterization of Pick's disease versus frontotemporal lobar degeneration with ubiquitin/TDP-43-positive inclusions. *Acta Neuropathol (Berl)* 2009; **117**: 429–444.
41. Josephs KA, Stroh A, Dugger B, Dickson DW. Evaluation of subcortical pathology and clinical correlations in FTLD-U subtypes. *Acta Neuropathol (Berl)* 2009; **118**: 349–358.
42. Kobayashi Z, Tsuchiya K, Arai T *et al.* Clinicopathological characteristics of FTLD-TDP showing corticospinal tract degeneration but lacking lower motor neuron loss. *J Neurol Sci* 2010; **298**: 70–77.
43. Yoshida M. Neuropathology of frontotemopral degeneration with ubiquitinated inclusions. *Brain Nerve* 2010; **61**: 1308–1318 (in Japanese with English abstract).
44. Tan C-F, Toyoshima Y, Kakita A, Takahashi H. Neuropathological similarities and differences between frontotemporal degeneration with ubiquitin inclusions and amyotrophic lateral sclerosis with dementia. *Brain Nerve* 2010; **61**: 1319–1327 (in Japanese with English abstract).
45. Geser F, Brandmeir NJ, Kwong LK *et al.* Evidence of multisystem disorder in whole-brain map of pathological TDP-43 in amyotrophic lateral sclerosis. *Arch Neurol* 2008; **65**: 636–641.
46. Nishihira Y, Tan C-F, Hoshi Y *et al.* Sporadic amyotrophic lateral sclerosis of long duration is associated with relatively mild TDP-43 pathology. *Acta Neuropathol (Berl)* 2009; **117**: 45–53.
47. Geser F, Stein B, Partain M *et al.* Motor neuron disease clinically limited to the lower motor neuron is a diffuse TDP-43 proteinopathy. *Acta Neuropathol (Berl)* 2011; **121**: 509–517.
48. Geser F, Martinez-Lage M, Kwong LK, Lee VM-Y, Trojanowski JQ. Amyotrophic lateral sclerosis, fronto-

temporal dementia and beyond: the TDP-43 disease. *J Neurol* 2009; **256**: 1205–1214.
49. Chen-Plotkin AS, Lee VM-Y, Trojanowski JQ. TAR DNA-binding protein 43 in neurodegenerative disease. *Nat Rev Neurol* 2010; **6**: 211–220.
50. Geser F, Lee VM-Y, Trojanowski JQ. Amyotrophic lateral sclerosis and frontotemporal lobar degeneration: a spectrum of TDP-43 ptroteinopathies. *Neuropathology* 2010; **30**: 103–112.

Acta Neuropathol
DOI 10.1007/s00401-012-1005-5

ORIGINAL PAPER

Coexistence of Huntington's disease and amyotrophic lateral sclerosis: a clinicopathologic study

Mari Tada · Elizabeth A. Coon · Alexander P. Osmand · Patricia A. Kirby · Wayne Martin · Marguerite Wieler · Atsushi Shiga · Hiroe Shirasaki · Masayoshi Tada · Takao Makifuchi · Mitsunori Yamada · Akiyoshi Kakita · Masatoyo Nishizawa · Hitoshi Takahashi · Henry L. Paulson

Received: 20 April 2012 / Revised: 14 June 2012 / Accepted: 15 June 2012

Abstract We report a retrospective case series of four patients with genetically confirmed Huntington's disease (HD) and sporadic amyotrophic lateral sclerosis (ALS), examining the brain and spinal cord in two cases. Neuropathological assessment included a polyglutamine recruitment method to detect sites of active polyglutamine aggregation, and biochemical and immunohistochemical assessment of TDP-43 pathology. The clinical sequence of HD and ALS varied, with the onset of ALS occurring after the mid-50's in all cases. Neuropathologic features of HD and ALS coexisted in both cases examined pathologically: neuronal loss and gliosis in the neostriatum and upper and lower motor neurons, with Bunina bodies and ubiquitin-immunoreactive skein-like inclusions in remaining lower motor neurons. One case showed relatively early HD pathology while the other was advanced. Expanded polyglutamine-immunoreactive inclusions and TDP-43-immunoreactive inclusions were widespread in many regions of the CNS, including the motor cortex and spinal anterior horn. Although these two different proteinaceous inclusions coexisted in a small number of neurons, the two proteins did not co-localize within inclusions. The regional distribution of TDP-43-immunoreactive inclusions in the cerebral cortex partly overlapped with that of expanded polyglutamine-immunoreactive inclusions. In the one case examined by TDP-43 immunoblotting, similar TDP-43 isoforms were observed as in ALS. Our findings suggest the possibility that a rare subset of older HD patients is prone to develop features of ALS with an atypical TDP-43

Electronic supplementary material The online version of this article (doi:10.1007/s00401-012-1005-5) contains supplementary material, which is available to authorized users.

M. Tada · H. L. Paulson (✉)
Department of Neurology, University of Michigan Health System, 109 Zina Pitcher Place, Biomedical Sciences Research Building, Room Number 4160, Ann Arbor, MI 48109-2200, USA
e-mail: henryp@med.umich.edu

M. Tada · M. Tada · M. Nishizawa
Department of Neurology, Brain Research Institute, University of Niigata, Niigata, Japan

M. Tada · A. Shiga · A. Kakita · H. Takahashi
Department of Pathology, Brain Research Institute, University of Niigata, Niigata, Japan

E. A. Coon
Department of Neurology, Mayo Clinic, Rochester, MN, USA

A. P. Osmand
Department of Medicine, University of Tennessee Graduate School of Medicine, Knoxville, TN, USA

P. A. Kirby
Department of Pathology, University of Iowa Carver College of Medicine, Iowa City, IA, USA

W. Martin · M. Wieler
Division of Neurology, University of Alberta, Alberta, Canada

H. Shirasaki
Shirasaki Clinic, Toyama, Japan

T. Makifuchi
Department of Clinical Research, Joetsu General Hospital, Niigata, Japan

M. Yamada
Department of Clinical Research, National Hospital Organization, Saigata National Hospital, Niigata, Japan

Published online: 27 June 2012

distribution that resembles that of aggregated mutant huntingtin. Age-dependent neuronal dysfunction induced by mutant polyglutamine protein expression may contribute to later-life development of TDP-43 associated motor neuron disease in a small subset of patients with HD.

Keywords Huntington's disease · Amyotrophic lateral sclerosis · Polyglutamine · TDP-43

Introduction

Huntington's disease (HD) is an inherited neurodegenerative disorder caused by an expanded CAG repeat that encodes an abnormally long polyglutamine stretch in the disease protein huntingtin [39]. Amyotrophic lateral sclerosis (ALS) is a neurodegenerative disorder that occurs sporadically or as a familial disorder. Both diseases are associated with abnormal protein accumulation: HD represents one of at least nine polyglutaminopathies [6], whereas ALS is characterized by the accumulation of the 43 kDa TAR-DNA-binding protein (TDP-43) [21]. Mutations in TDP-43 have been identified in sporadic and familial ALS, and thus ALS is now recognized as one of several TDP-43 proteinopathies [2, 13, 37, 44].

Despite the fact that HD and ALS are relatively rare and clinically distinct, more than ten patients with HD have been reported to show ALS-like clinical features [14, 25, 27, 31, 32]; the coincidental occurrence of both diseases, however, is predicted to be only 2–6 cases per billion [9, 15]. Notwithstanding the recent exclusion of the HD disease gene as a risk factor for ALS [17, 29], these cases raise the question: does mutant huntingtin have a deleterious effect on motor neurons that predisposes HD mutation carriers to motor neuron degeneration? To address this question, we first must define the pathologic features of such cases. Although the pathology of a single case with concurrent familial ALS and HD has been reported [31], there is no pathologic report of sporadic ALS occurring in genetically confirmed HD.

Here we report three individuals with confirmed HD and one HD mutation carrier who developed ALS. We performed pathologic and biochemical studies in two cases to assess whether dual pathological findings of ALS and HD are indeed present, and whether they show characteristic features that suggest effects of mutant huntingtin on ALS pathology.

Patients and methods

Patients

Patients were referred to the Departments of Neurology at the University of Iowa (case 1), National Hospital of Saigata (case 2), University of Michigan (case 3), and University of Alberta (case 4). Written informed consent for autopsy including use of tissue for research purposes was obtained from next of kin. The present study was approved by the institutional review boards of the Iowa University School of Medicine, IA and Niigata University School of Medicine and Saigata National Hospital, Niigata, Japan.

Neuropathologic techniques and immunohistochemistry

Neuropathologic examination was performed in cases 1 and 2. Formalin-fixed, paraffin-embedded sections were prepared from brain and spinal cord and stained with hematoxylin and eosin and Klüver–Barrera (K.B.) staining methods. Sections were also immunostained using polyclonal antibodies against phosphoserines 409 and 410 of TDP-43 (pS409/410-2; Cosmo Bio Co., Ltd., Tokyo, Japan; 1:4,000), TDP-43 (10782-2-AP; Protein Tec Group Inc., Chicago, IL, USA; 1:4,000) and ubiquitin (Dako, Glostrup, Denmark; 1:1,000), and monoclonal antibodies against expanded polyglutamine (1C2) (Chemicon, Temecula, CA, USA; 1:10,000), huntingtin (EM48) (MAB5374; Chemicon, Temecula, CA, USA; 1:100) and p62 (3/p62 LCK LIGAND; BD biosciences, San Jose, CA, USA; 1:500). Four-μm-thick sections were pre-treated with formic acid for 1C2 immunostaining, or in a microwave oven in a 10-mM citrate buffer (pH 6.0) for other antibodies. Immunolabeling was detected using the avidin–biotin-peroxidase complex method with Vectastain ABC kit (Vector, Burlingame, CA, USA), and visualized with diaminobenzidine/H_2O_2 solution. Counterstaining was carried out with hematoxylin. Double-label immunofluorescence was performed on sections of spinal cord (case 1 and 2), motor cortex (case 1) and frontal cortex (case 2), using antibodies against pS409/410 of TDP-43 (1:2,000) or TDP-43 (1:2,000) together with 1C2 (1:2,000) or EM48 (1:50). Secondary antibodies were Alexa Fluor 488 goat anti-rabbit IgG and Alexa Fluor 568 or 555 goat anti-mouse IgG (Molecular Probes; 1:1,000). Nuclei were stained with 4,6-diamidino-2-phenylindole (DAPI). Sections were analyzed by confocal laser-scanning microscope (LSM510-V4.0; Carl Zeiss Co., Ltd.). To detect active sites of polyglutamine aggregation, 40-μm-thick sections were cut from spinal cord and motor cortex of case 1 and control case with a vibrating microtome and immunostained with the polyglutamine peptide recruitment method as described previously [10, 24]. Briefly, sections were immunostained using a biotinylated polyglutamine peptide containing approximately 30 glutamine residues. Immunolabeling was detected using the avidin–biotin-peroxidase complex method with Vectastain ABC kit and visualized with diaminobenzidine/H_2O_2 solution.

Fractionation of frozen tissues and TDP-43 immunoblotting

Protein lysates were generated as described [8, 38] from frontal, motor and temporal cortices of case 2, one ALS, two HD and two control brains. Briefly, frozen tissues were homogenized in buffer A [10 mM Tris–HCl (pH 7.5), 1 mM ethylene glycol-bis[-β-amio-ethylether]-tetra-acetic acid, 1 mM dithiothreitol, 10 % sucrose] and centrifuged at 25,000×*g* for 30 min at 4 °C. The resulting pellets were extracted in buffer A containing 1 % Triton X-100 and centrifuged at 180,000×*g* for 30 min at 4 °C. These pellets were subsequently homogenized in buffer A containing 1 % sarcosyl, incubated for 1 h, and centrifuged at 180,000×*g* for 30 min at 22 °C. The sarkosyl-insoluble pellets were solubilized in 8 M urea buffer. After centrifugation at 25,000×*g* for 30 min at 22 °C, the supernatants were separated by sodium dodecyl sulfate–polyacrylamide gel electrophoresis and analyzed by immunoblotting with anti-TDP-43 polyclonal antibody (1:2,000) and anti-pS409/410 of TDP-43 monoclonal antibody (Cosmo Bio Co., Ltd; 1:2,000). Detailed case information is in Online Resource 1.

Gene analysis of TARDBP, progranulin and C9ORF72 genes

High-molecular weight genomic DNA was extracted. We amplified all the exons of TARDBP (NM_007375.3) and progranulin (NM_002087.2) genes with use of a series of primers, followed by sequence reaction. For screening of GGGGCC repeat expansion in C9ORF72 (NM_018325.2), fluorescence fragment length analysis of PCR fragments was performed on an ABI 3130xl genetic analyzer (Applied Biosystems, Foster City, CA, USA) and Peak Scanner software v1.0 (Applied Biosystems) according to previously described methods [3].

Results

Case 1

In her mid-50's the patient, who had a family history suggestive of HD, developed chorea in all limbs, mild irregularities in speech, emotional lability and difficulty concentrating. Neurological examination at age 58 revealed subtle dysarthria, choreiform movements of the face and limbs, slowed and irregular alternating hand movements, and lower limb hyperreflexia without spasticity. No muscle weakness or atrophy was noted. Mild caudate atrophy was seen on magnetic resonance imaging (MRI), and HD genetic testing revealed a pathogenic CAG repeat of 46 in the *HTT* gene, establishing the diagnosis of HD. One year later she developed right hand weakness. A brachial plexus lesion was suspected, prompting surgery to remove a cervical rib, but her weakness progressed and soon involved all limbs and neck. At age 60, she was noted to have distal atrophy of upper limbs, fasciculations in all limbs, diffuse hyperreflexia and extensor plantar responses. Electromyography (EMG) revealed extensive denervation in both upper extremities. Except for having HD, she fulfilled a diagnosis of probable ALS according to El Escorial criteria [1], and she was placed on riluzole. She died of respiratory weakness at age 61.

Case 2

The patient developed chorea and cognitive changes in her mid-30's. Her father, sister and numerous other relatives had shown similar symptoms. She was referred to the neurology clinic at age 44 where an examination revealed choreiform movements of the face, neck and limbs without weakness or muscle atrophy. Caudate atrophy was seen on the brain computed tomography consistent with HD, and the diagnosis was confirmed with a CAG repeat of 47. Her cognitive impairment progressed and at age 48, she was bed-ridden. Examination revealed bilateral extensor plantar responses, rigidity and chorea. At age 57, extensor plantar responses were still evident but she was hypotonic with no involuntary or volitional limb movements. MRI showed brain atrophy with areas of signal hyperintensity in the cerebral white matter on T2-weighted images. She developed progressive respiratory decline and died at age 58.

Case 3

The patient was referred for neurological evaluation of HD at age 62. Numerous relatives, including three siblings, her mother and maternal grandmother, were affected with HD but there was no family history of ALS. She had developed chorea in her mid-50's, which slowly worsened and was later accompanied by incoordination as well as cognitive and personality changes. Examination revealed choreiform movements in all limbs, trunk and face with hand clumsiness, postural instability and lower limb hyperreflexia. No speech or swallowing impairment, weakness or muscle atrophy was noted at this point. Genetic analysis confirmed the diagnosis of HD with a CAG repeat of 42. At age 66 she developed dysarthria and dysphagia, and within several months was anarthric and unable to swallow. EMG revealed extensive denervation in upper and lower extremities and thoracic paraspinal muscles. Further laboratory tests were negative including anti-GM1 antibodies. Except for having HD, she fulfilled a diagnosis of clinically probable, laboratory-supported ALS according to El Escorial criteria [1].

Case 4

The patient was referred at age 48 for neurological evaluation following predictive testing for HD that revealed an expanded CAG repeat of 39. His father had developed symptoms of HD in his mid-50's and died at age 66. An examination revealed no neurological deficits at the time of predictive testing. At age 56 he developed dysarthria, which progressed over the following year such that his speech became nearly incomprehensible and was accompanied by drooling and nasal regurgitation. An examination revealed pseudobulbar affect with emotional incontinence, hyperactive jaw jerk and tongue atrophy. Mild weakness was evident in all limbs along with fasciculations in the arms, spasticity, diffuse hyperreflexia and extensor plantar responses. MRI revealed signal changes in the corticospinal pathways bilaterally from motor cortex to brainstem. EMG revealed acute and chronic denervation in multiple muscle groups including paraspinal muscles. A diagnosis of definite ALS was made according to El Escorial criteria [1]. At age 58, he required a keyboard to facilitate communication. His gait became wide-based with a steppage and spastic quality, requiring a walker.

Neuropathologic findings, case 1

The brain weighed 1,346 g before fixation and had selective atrophy of the precentral gyrus. Coronal brain sections revealed atrophy of the neostriatum without gross atrophy of the cerebral cortices (Fig. 1a). Marked myelin pallor was seen in the corticospinal tracts in the brainstem and spinal cord (Fig. 1b). Neuronal loss and gliosis were evident in the spinal anterior horn, most marked in the cervical cord (Fig. 1c). Bunina bodies were occasionally found in the remaining anterior horn cells (Fig. 1d) and in neurons of the hypoglossal nucleus. The motor cortex showed severe loss of pyramidal neurons, including Betz cells, and gliosis was evident (Fig. 1e). The remaining cerebral cortex was well preserved (Fig. 1f). Moderate neuronal loss and gliosis were evident in the caudate nucleus (Fig. 1g) and dorsal putamen (Vonsattel grading; grade 2) [42].

Immunohistochemistry revealed 1C2-immunoreactive (ir) neuronal intranuclear inclusions (NIIs) and neuronal cytoplasmic inclusions (NCIs) as well as TDP-43-ir NCIs in diverse areas of the CNS (Table 1). NIIs and NCIs were observed with anti-huntingtin (EM48) and anti-polyglutamine (1C2) antibodies in spinal anterior horn cells (Fig. 1h, i) and neurons of the entire cerebral cortex including motor cortex (Fig. 1j, k), predominantly in layer V–VI with occasional round or ellipsoid inclusions in the neuropil (Fig. 1l). Polyglutamine recruitment staining in the spinal cord and motor cortex revealed aggregation foci distributed in the cytoplasm and proximal dendrites of anterior horn cells (Fig. 1m) and pyramidal neurons (Fig. 1n), whereas no aggregation was observed in a normal control (Fig. 1o).

Using TDP-43 antibody, only a few NCIs were observed in the temporal cortex and none in dentate granular cells and Ammon's horn despite widespread NCIs in the motor and parietal cortex. TDP-43-ir NCIs varied in shape, adopting filamentous skein-like (Fig. 1p, r), dash-like (Fig. 1q), circumferential (Fig. 1s), and round (Fig. 1t) patterns. TDP-43-ir cytoplasmic inclusions were also seen in glial cells in motor cortex, adjacent white matter, and corticospinal tract (Fig. 1u). In the spinal cord and motor cortex, anti-p62 and anti-ubiquitin antibodies labeled NCIs (Fig. 1v, w) and GCIs (Fig. 1x, y) that were similarly shaped but less frequent than the TDP-43-ir inclusions.

Neuropathologic findings, case 2

The brain weighed 708 g before fixation, showing severe global cerebral atrophy. Coronal brain sections revealed severe cortical and white matter atrophy with marked myelin pallor in the entire cerebrum and marked atrophy of the neostriatum (Fig. 2a). Myelin pallor was also seen in the corticospinal tract in the brainstem and spinal cord. Neuronal loss and gliosis were evident in the hypoglossal nucleus and spinal anterior horn, especially in cervical and thoracic segments (Fig. 2b). Bunina bodies (Fig. 2c) and round inclusions (Fig. 2d) were occasionally found in the remaining anterior horn cells and in neurons of brainstem motor nuclei. Neuronal loss and gliosis were severe throughout the cerebral cortex especially in layers V and VI (Fig. 2e). Myelinated fibers were sparse and gliosis was evident in the adjacent cerebral white matter (Fig. 2f). Neuronal loss and gliosis were severe in the caudate nucleus (Fig. 2g), and moderate in the putamen and globus pallidus (Vonsattel grading; grade 4) [42].

Immunohistochemistry revealed 1C2-ir NIIs and NCIs as well as TDP-43-ir NCIs in diverse areas of the CNS (Table 1). Numerous NIIs and neuropil inclusions were observed with 1C2 and EM48 antibodies throughout the cerebral cortex, accentuated in frontal and motor cortex and more frequent in layers II and III (Fig. 2h, i). Scattered glial intranuclear inclusions were also present in the cerebral white matter (Fig. 2j). 1C2-ir NIIs and NCIs were also seen in spinal anterior horn cells (Fig. 2k, l).

With TDP-43 antibody, many NCIs were detected in the cerebral cortex, particularly in the frontal cortex, mainly in layer II with numerous dot-like short neurites and scattered long neurites (Fig. 2m, n). Numerous NCIs were also seen in other regions including the dentate gyrus (Fig. 2o), yet no NCI in the Ammon's horn. Many round or skein-like TDP-43-ir NCIs were detected in the remaining lower

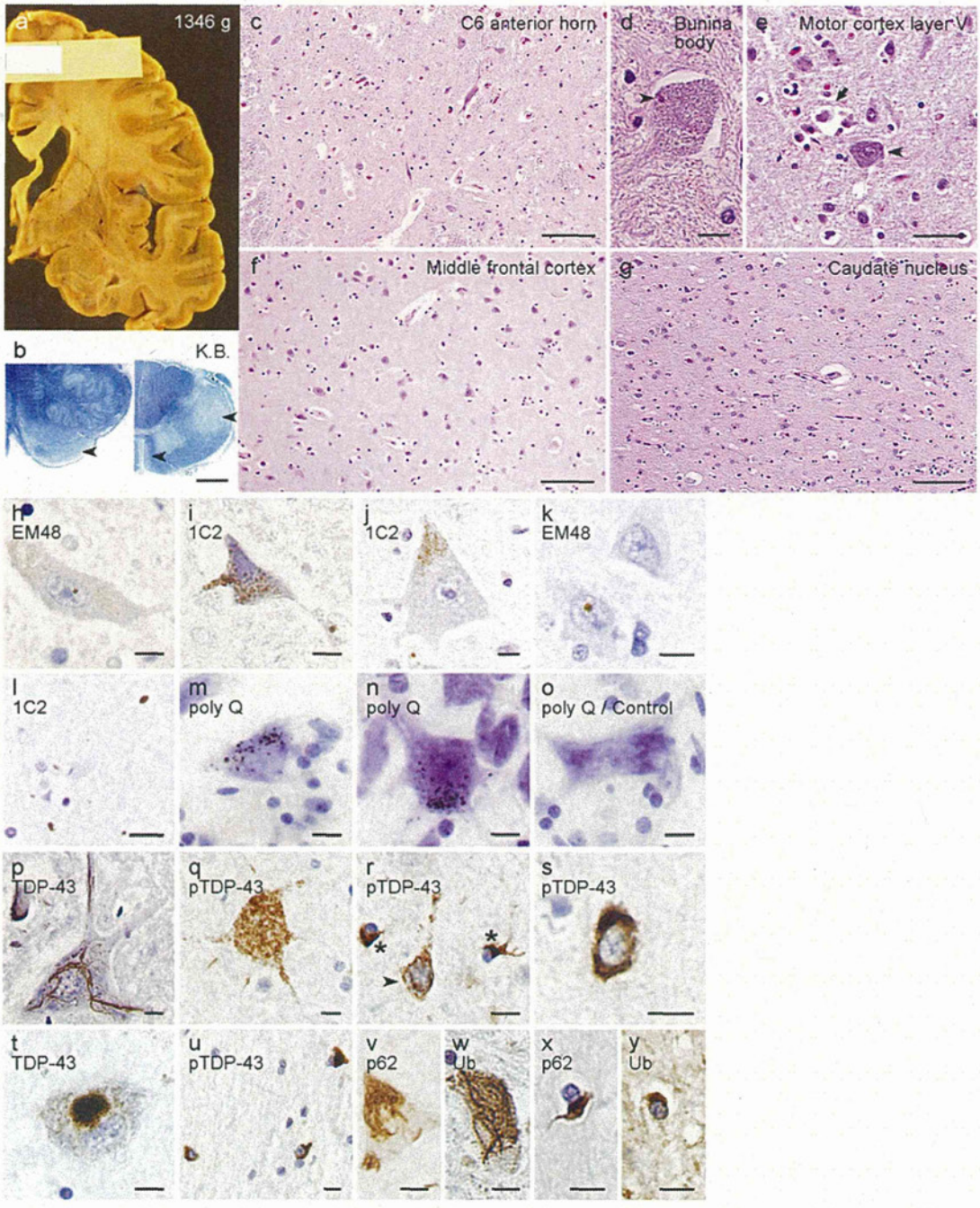

Fig. 1 Neuropathologic findings, case 1. Coronal section at the level of the lenticular nucleus (**a**). Transverse sections of the ventral medulla and spinal cord at the C5 level. Degeneration of corticospinal tracts (*arrowheads*) (**b**). Low-power view of the spinal anterior horn at the C6 level (**c**). Bunina body (*arrowhead*) in a cervical anterior horn cell (**d**). Betz cell (*arrowhead*) and a Betz cell-sized hole containing lipofuscin-laden macrophages (*arrow*) indicating that Betz cells had presumably disappeared (**e**). The deeper layers of middle frontal cortex (**f**). Caudate nucleus (**g**). Klüver-Barrera staining (**b**). Hematoxylin and eosin (**c**–**g**). *Bar*s 2 mm (**b**), 100 μm (**c**, **f**, **g**), 10 μm (**d**), 50 μm (**e**). Expanded polyglutamine (1C2)- and huntingtin (EM48)-immunoreactive (ir) inclusions (**h**–**l**). Neuronal intranuclear (**h**) and cytoplasmic (**i**) inclusions in cervical anterior horn cells. Granular inclusions in Betz cell (**j**). An intranuclear inclusion in a pyramidal neuron in motor cortex (**k**). Neuropil inclusions in layer V of motor cortex (**l**). Polyglutamine recruitment methods (**m**–**o**). Aggregation foci in an anterior horn cell (**m**) and a pyramidal neuron in motor cortex (**n**). Anterior horn cell from a control case (**o**). *Bars* 10 μm (**h**–**k**, **m**–**o**), 20 μm (**l**). TDP-43-ir neuronal and glial inclusions (**p**–**u**). Skein-like inclusions in a cervical anterior horn cell (**p**). Dash-like inclusions in Betz cell (**q**) and a pyramidal neuron (**r**, *arrowhead*). Glial cytoplasmic inclusions (GCIs) in motor cortex (**r**, *asterisks*). Circumferential inclusion in a putaminal neuron (**s**). Round inclusion in substantia nigra (**t**). GCIs in the white matter adjacent to motor cortex (**u**). p62-ir or ubiquitin-ir skein-like inclusions in spinal anterior horn cells (**v**, **w**) and GCIs (**x**, **y**). *Bar* 10 μm (**p**–**y**)

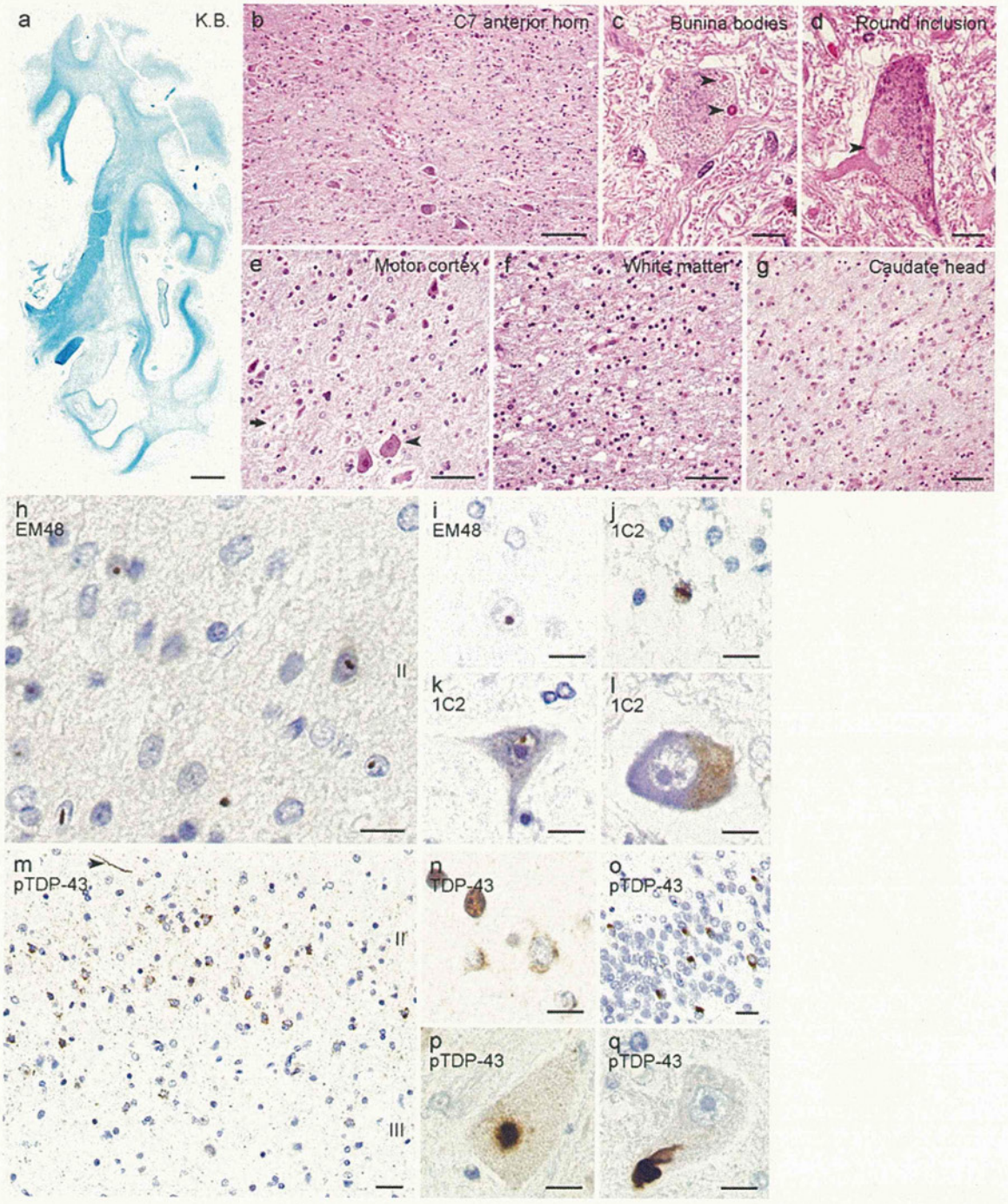

Fig. 2 Neuropathologic findings, case 2. Coronal section at the level of the lenticular nucleus (**a**). Low-power view of the spinal anterior horn at the C7 level (**b**). Bunina bodies (**c**, *arrowheads*) and a round inclusion (**d**, *arrowhead*) in cervical anterior horn cells. Low-power view of motor cortex with atrophic Betz cells (*arrowhead*) and a Betz cell-sized hole containing lipofuscin-laden macrophages (**e**, *arrow*). High-power view of the white matter adjacent to motor cortex (**f**). Low-power view of caudate head (**g**). Klüver–Barrera staining (**a**). Hematoxylin and eosin (**b**–**g**). *Bars* 5 mm (**a**), 100 μm (**b**), 10 μm (**c**, **d**), 50 μm (**e**, **g**), 20 μm (**f**). Expanded polyglutamine (1C2)- or huntingtin (EM48)-immunoreactive (ir) inclusions (**h**–**l**). Intranuclear and neuropil inclusions in layers II of motor cortex (**h**). Intranuclear inclusion in a pyramidal neuron in motor cortex, layer V (**i**). Intranuclear inclusion in a glial cell in the white matter adjacent to motor cortex (**j**). Intranuclear (**k**) and cytoplasmic granular (**l**) inclusions in lumbar anterior horn cells. *Bar* 10 μm (**h**–**l**). TDP-43-ir inclusions (**m**–**q**). Neuronal cytoplasmic inclusions (NCIs) with fine dot-like neuropil staining and a long neurite (*arrowhead*) in frontal cortex, layer II (**m**). Nuclei of neurons with NCIs were unstained with phosphorylation-independent TDP-43 antibody. Frontal cortex layer II (**n**). Multiple NCIs in the granular cells of the dentate gyrus (**o**). Round inclusion in a cervical anterior horn cell (**p**). Skein-like inclusions in trigeminal motor nucleus (**q**). *Bars* 20 μm (**m**, **o**), 10 μm (**n**, **p**, **q**)

Table 1 Distribution and severity of neuronal loss and pTDP-43 and 1C2 lesions in Case 1 and 2

	Case 1				Case 2			
	Neuronal loss	pTDP-43 NCIs	1C2 NI staining[a]	1C2 NC staining[b]	Neuronal loss	pTDP-43 NCIs	1C2 NI staining[a]	1C2 NC staining[b]
Cerebral cortex (II–III/IV–VI)								
Frontal cortex	−/−	±/±	+/++	+/++	++/+++	+++/+	+++/+++	++/++
Motor cortex	++/+++	+++/+++	+/++	+/++	+++/+++	++/+	+++/+++	++/++
White matter[c]		++				+		
Parietal cortex	−/−	++/++	++/++	+/++	++/+++	+/±	++/++	+/+
Temporal cortex	−/−	−/±	+/++	+/++	++/+++	++/+	+++/++	+/+
Occipital cortex	−/−	−/−	+/++	+/++	++/+++	+/±	++/++	+/+
Subcortical area								
Ammon	−	−	±	−	−	−	+	±
Dentate gyrus	−	−	±	−	−	++	±	−
Amygdaloid nucleus	NA	NA	NA	NA	−	+	+	+
Putamen	++	+	+++	++	+++	+	++	++
Caudate nucleus	++	−	++	+	+++	±	++	+
Globus pallidus	+	−	±	±	+	±	±	±
Internal capsule[c]		+				+		
Thalamic nuclei	−	+−++	+	+	−	++	++	++
Brain stem								
Periaqueductal gray	−	±	±	−	−	−	+	+
Oculomotor nucleus	−	−	−	−	−	±	−	++++
Red nucleus	−	±	−	−	NA	NA	NA	NA
Substantia nigra	−	±	±	+	+	+	±	±
Pyramidal tract of midbrain[c]		++				±		
Locus ceruleus	−	−	−	±	−	−	±	+
Trigeminal motor nucleus	−	±	−	−	−	+++	−	±
Pontine nuclei	−	+	+	++	−	+	++	+++++
Pyramidal tract of pons[c]		+				±		
Hypoglossal nucleus	−	+++++	−	−	+	++++	−	−
Ambiguus nucleus	NA	NA	NA	NA	±	++++	−	−
Dorsal nucleus of vagus	−	−	−	−	−	−	−	±
Reticular formation	−	±	±	±	−	±	±	+
Inferior olivary nucleus	−	+	±	++	−	±	−	−
Pyramis[c]		++				−		
Cerebellum								
Cortex	−	−	−	−	+	−	±	+
Dentate nucleus	−	−	±	++	+	−	++	++++
Cerebellar white matter[c]		+				±		
Spinal cord								
Anterior horn	++−+++	+++++	±	±	++	+++++	±	++++
Corticospinal tract[c]		±−+				±		
Intermediate lateral nucleus	−	±	±	−	−	−	−	−

Table 1 continued

	Case 1				Case 2			
	Neuronal loss	pTDP-43 NCIs	1C2 NI staining[a]	1C2 NC staining[b]	Neuronal loss	pTDP-43 NCIs	1C2 NI staining[a]	1C2 NC staining[b]
Clarke's column	−	−	±	±	+	−	±	±
Posterior horn	−	±	±	±	−	−	+	+

Percentage of neurons expressing pTDP-43 or expanded polyglutamine (1C2) immunoreactivity; −,0 %; ±, ≤3 cells/section; +, <1 %; ++, 1–10 %; +++, 10–30 %; ++++, 30–60 %; +++++, >60 %

NCIs neuronal cytoplasmic inclusions, *NA* not available

[a] Neuronal intranuclear diffuse and aggregated staining

[b] Neuronal cytoplasmic diffuse and aggregated staining

[c] pTDP-43 immunoreactive glial pathology severity; −, none; ±, ≤3 cells/section; +, rare; ++, occasional; +++, many

motor neurons of the spinal anterior horn (Fig. 2p) and the trigeminal motor (Fig. 2q), hypoglossal and ambiguus nuclei. No TDP-43-ir NIIs were detected in the CNS. Based on the classification system for FTLD–TDP, the TDP-43 cortical pathology of case 2 could be considered type A [18, 19, 33] (i.e. numerous short dystrophic neurites and NCIs concentrated primarily in neocortical layer II), although the presence of long neurites and dot-like neuropil staining is atypical.

Double-label immunofluorescence, cases 1 and 2

TDP-43 did not co-localize with expanded polyglutamine or mutant huntingtin in NCIs, NIIs, GCIs or neuropil inclusions (Fig. 3a–l). In contrast, separate TDP-43-ir NCIs and 1C2- or EM48-ir NIIs or NCIs did coexist in a small number of neurons in the spinal cord and motor and frontal cortex (Fig. 3j–l). In these areas, approximately half of the TDP-43-ir NCIs and several GCIs were immunoreactive for p62. Less frequently, NCIs and GCIs were also immunoreactive for ubiquitin (not shown).

TDP-43 immunoblot analysis, case 2

In lysates examined from case 2, ALS, HD and control cases, anti-TDP-43 antibody showed a ~43-kDa band consistent with non-phosphorylated TDP-43, with an additional ~45-kDa band being observed only in case 2 and the ALS case. Anti-phosphorylated TDP-43 antibody detected a ~45-kDa band and ~26-kDa fragment, as well as an indistinct ladder-like smear in case 2 and the ALS case, but not in the HD or control cases (Fig. 4). In addition, the pattern of ~26-kDa bands corresponding to TDP-43 fragments was similar in case 2 and the ALS case, consistent with what has been described in ALS [8] (data not shown).

Gene analysis of TARDBP, progranulin and C9ORF72, case 2

Case 2 showed no mutation in the TARDBP or progranulin gene, and no expansion of the C9ORF72 hexanucleotide repeat.

Discussion

Here we reported clinical and neuropathologic features in a series of patients with genetically confirmed symptomatic HD (three cases) or possessing the HD mutation (one case) who also manifested clinical and/or pathologic features of ALS. Neuropathological and biochemical evaluation of the spinal cord and brain from two patients confirmed the coexistence of pathological features of HD and ALS. Our findings suggest that the HD pathogenic process can involve motor neurons while also indicating that, in these two HD cases, TDP-43-associated processes contribute to motor neuron degeneration, as in typical ALS.

Pathologic findings of HD and ALS coexisted in both examined cases. Both showed obvious upper and lower motor neuron loss with Bunina bodies and ubiquitin-ir skein-like inclusions in remaining lower motor neurons, which are characteristic of ALS [15, 28], as well as neuronal loss and gliosis in the neostriatum together with polyglutamine inclusion-containing neurons, which are hallmarks of HD [9, 11, 43]. A single reported autopsy case with HD and familial ALS likewise had these characteristics of ALS and HD, but also showed degeneration of posterior columns and dorsal spinocerebellar tracts, which was not present in our cases [31].

As shown in Table 1, TDP-43-ir NCIs were found in many regions beyond the affected lower motor nuclei and motor cortex. This pattern represents a broader distribution than seen in classical sporadic ALS, more reminiscent of a

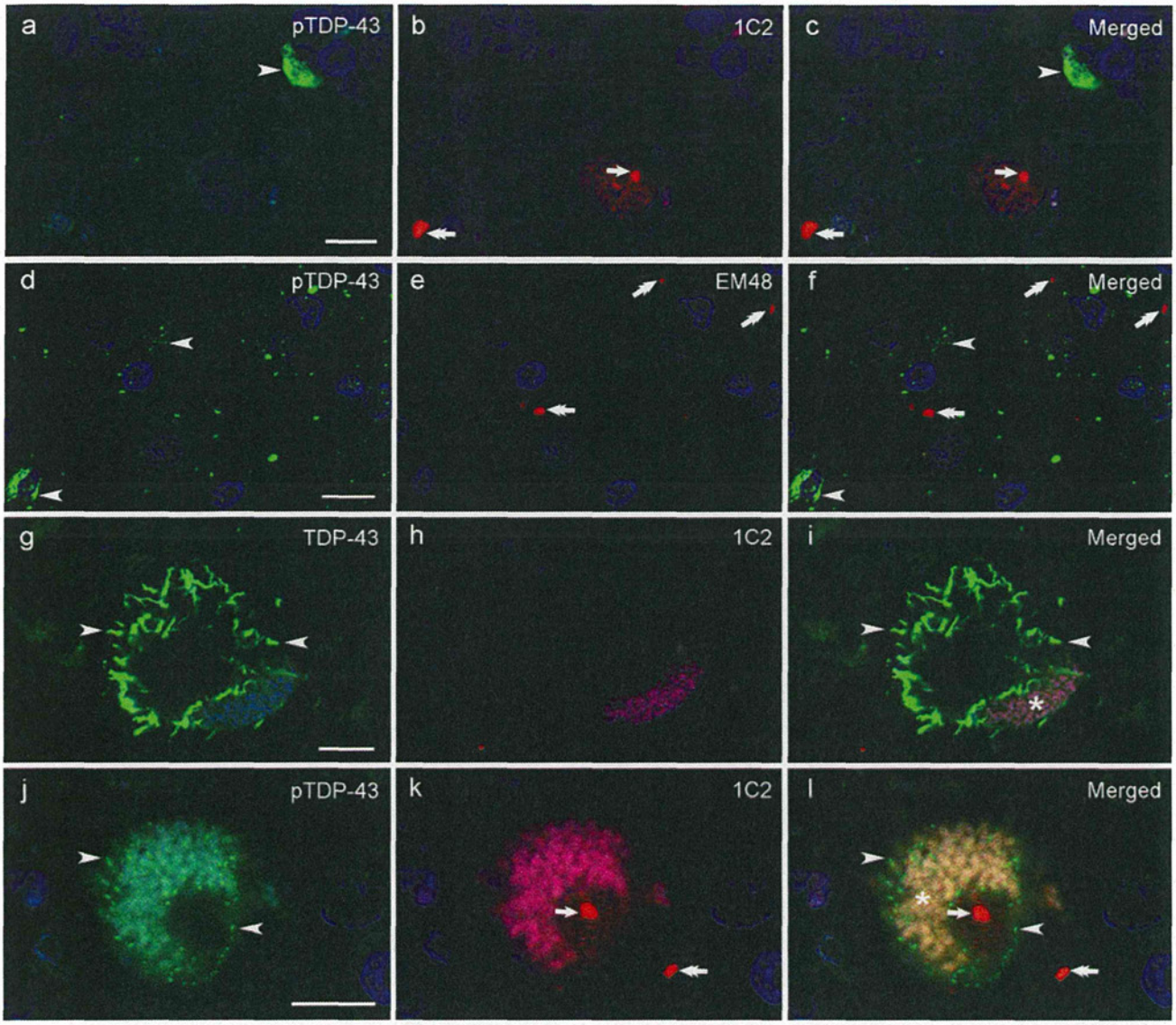

Fig. 3 Association of TDP-43 and expanded polyglutamine or huntingtin. Co-immunofluorescence staining for TDP-43 [*green*; p409/410 TDP-43 (**a–f**, **j–l**), TDP-43 (**g–i**)] and expanded polyglutamine [*red*; 1C2 (**a–c**, **g–l**)] or mutant huntingtin [*red*; EM48 (**d–f**)]. TDP-43-positive, 1C2 or EM48-negative neuronal cytoplasmic inclusions (*arrowheads*) and TDP-43-negative, 1C2 or EM48-positive neuronal intranuclear inclusions (*arrow*) and neuropil inclusions (*double arrows*) in layer V of motor cortex (**a–c**) and layer II of frontal cortex (**d–f**). TDP-43-positive, 1C2-negative skein-like inclusions (*arrowheads*) in a lumbar anterior horn cell (**g–i**). TDP-43-positive, 1C2-negative wisp-like cytoplasmic inclusions (*arrowheads*) and a TDP-43-negative, 1C2-positive neuronal intranuclear inclusion (*arrow*) coexisting in the same cervical anterior horn cell (**j–l**). The diffuse and irregular structure seen in all *green*, *red* and *blue* fluorescent channels represents autofluorescence (*asterisks*; **i**, **l**). Nuclei were stained with DAPI; *blue*. *Bar* 10 μm (**a**, **d**, **g**, **j**). **a–c** Case 1, **d–l** case 2

"type 2 ALS" pattern of TDP-43 pathology [22]. The pattern, however, also displayed features atypical of type 2 ALS. For example, TDP-43-ir NCIs were absent from the dentate gyrus in case 1 and Ammon's horn in both cases 1 and 2. In these regions, TDP-43-ir NCIs have been observed in over 85 % of patients with type 2 ALS [22]. In case 2, only a small number of TDP-43-ir NCIs were seen in the amygdaloid nucleus, a region in which numerous NCIs appear in typical type 2 ALS [7]. In both our cases, 1C2-ir neurons were also rare in these regions. Unlike type 2 ALS [22] our cases lacked prominent TDP-43 pathology in temporal cortex. Instead, TDP-43-ir NCIs were abundant in the parietal cortex in case 1 and frontal cortex in case 2, where 1C2-ir neurons were also more frequently observed than in temporal cortex. Thus, the distribution of TDP-43 in our HD/ALS cases resembles a classical ALS distribution (type 1 [22]) with a superimposed, atypical cortical distribution that may mirror the distribution of 1C2-ir pathology.

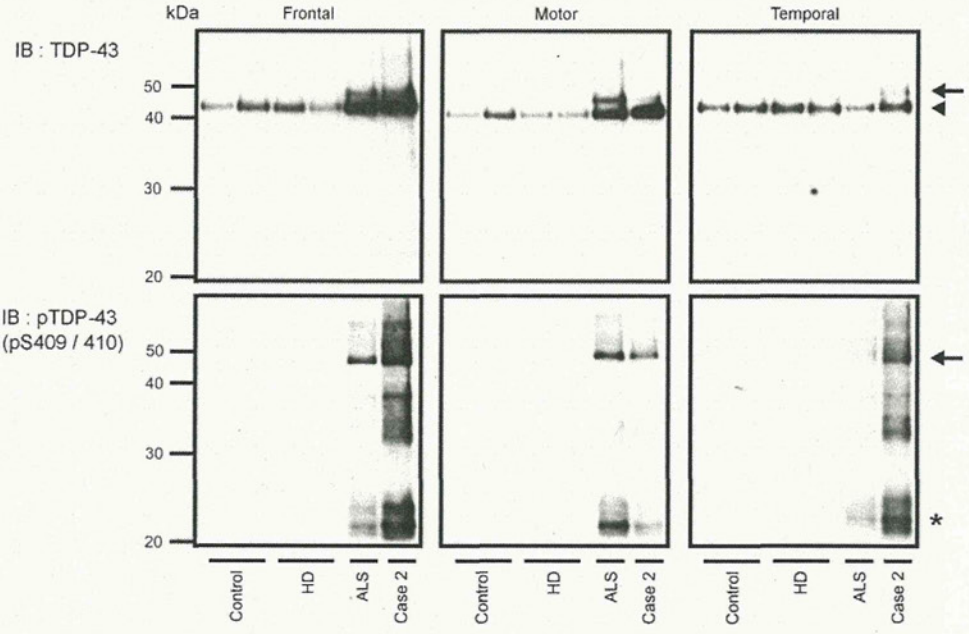

Fig. 4 TDP-43 immunoblot analysis, case 2. Immunoblot analysis of the sarkosyl-insoluble, urea-soluble fraction from case 2 and one ALS, two HD and two control brains (frontal, motor and temporal cortices). Blots were probed with antibodies to TDP-43 (*upper panels*) and phosphorylated TDP-43 (pS409/410) (*lower panels*). *Arrows* and an *arrowhead* indicate ~45 and 43-kDa full-length isoforms of TDP-43, respectively, and an *asterisk* indicates a fragment of TDP-43

However, because some regions with abundant 1C2-ir neurons displayed few or no TDP-43-ir NCIs and lower motor nuclei had abundant TDP-43-ir NCIs yet few were 1C2-ir neurons, we could not conclude from the present data that the distribution of TDP-43 pathology was directly affected by mutant huntingtin.

In neurons of the motor cortex and lower motor neurons, we also detected expanded polyglutamine inclusions and aggregation foci which suggest ongoing huntingtin aggregation [10, 24]. Although 1C2-ir NIIs in anterior horn cells have been described in HD [11, 43], we confirmed their presence and, using the polyglutamine recruitment technique, found evidence for active polyglutamine aggregation in motor neurons. Thus, we conclude that TDP-43-dependent and mutant huntingtin-dependent pathogenic processes likely occur simultaneously in motor neurons in such cases.

We found neurons in which separate TDP-43-ir NCIs and 1C2/EM48-ir NIIs or NCIs coexisted, but in such neurons we failed to observe co-localization of mutant huntingtin protein and TDP-43 within the same inclusions in our two cases. We also immunohistochemically examined the frontal cortex and neostriatum of other 11 patients with HD who did not show clinicopathological features associated with ALS [10 male, 1 female, age; 57.8 (27–82) years, CAG repeat; 44.1 (43–47) in available 7 patients] and the spinal cord of 7 of the patients with an anti-pTDP-43 antibody. We observed only a small number of TDP-43-ir neuropil inclusions similar to mutant huntingtin neuropil inclusions in the deeper layers of frontal cortex of nine patients and much fewer in the neostriatum but no inclusions in the spinal cord. In contrast, others reported frequent co-localization of these two proteins in neuropil inclusions and dystrophic neurites in the cortex and neostriatum of HD cases [34]. This discrepancy may reflect differences in the cases examined or in methods of tissue preparation.

Motor neuron degeneration is recognized in other polyglutamine diseases: for example, spinobulbar muscular atrophy is a form of motor neuron degeneration [36], and three patients with spinocerebellar ataxia type 2 (SCA2) and one with SCA6 have been described with concomitant ALS [5, 12, 20, 23]. Once TDP-43 was discovered to be a key component in ALS, TDP-43-ir NCIs were detected in neurons from various areas of SCA2 disease brain [4, 40] and in lower motor neurons and axons in patients with Machado-Joseph disease (also known as SCA3) [35, 38]. Similar to our two cases, in reported cases, co-localization of TDP-43 and mutant polyglutamine proteins has not been observed and coexistence of these proteins in the same neuron is infrequent [38, 40]. In addition, expanded CAG repeats in the SCA2 disease gene are associated with increased risk for ALS [4, 30, 41]. Although the pathophysiological mechanism remains unclear, intermediate expansion in the SCA2 disease protein ATXN2 has been suggested to perturb neuronal proteostasis thereby favoring TDP-43 mislocalization [4, 30]. Since two studies examining CAG repeat length in the HD disease gene in sporadic ALS versus controls have concluded that, unlike the SCA2 gene, the HD disease gene is not a risk factor for ALS [17, 29], we cannot exclude the possibility that our patients suffer from both HD and ALS by chance alone. Certainly, the abundance of TDP-43-ir NCIs in our two cases is not a common feature of typical HD. Yet in a rare subset of HD patients, mutant huntingtin may predispose